First publ. in: International journal of cancer ; 123 (2008), 8. - pp. 1797–1806

Thiazolides inhibit growth and induce glutathione-*S*-transferase Pi (GSTP1)-dependent cell death in human colon cancer cells

Joachim Müller[1]*, Daniel Sidler[2], Ueli Nachbur[2], Jonathan Wastling[3,4], Thomas Brunner[2] and Andrew Hemphill[1]*

[1]*Institute of Parasitology, University of Berne, Länggass-Strasse 122, CH-3012 Berne, Switzerland*
[2]*Institute of Pathology, Division of Immunopathology, University of Berne, Murtenstrasse 31, 3010 Berne, Switzerland*
[3]*Department of Pre-Clinical Science, Faculty of Veterinary Science, University of Liverpool, Liverpool, United Kingdom*
[4]*Department of Veterinary Pathology, Faculty of Veterinary Science, University of Liverpool, Liverpool, United Kingdom*

Thiazolides are a novel class of broad-spectrum anti-infective drugs with promising *in vitro* and *in vivo* activities against intracellular and extracellular protozoan parasites. The nitrothiazole-analogue nitazoxanide (NTZ; 2-acetolyloxy-*N*-(5-nitro 2-thiazolyl) benzamide) represents the thiazolide parent compound, and a number of bromo- and carboxy-derivatives with differing activities have been synthesized. Here we report that NTZ and the bromo-thiazolide RM4819, but not the carboxy-thiazolide RM4825, inhibited proliferation of the colon cancer cell line Caco2 and nontransformed human foreskin fibroblasts (HFF) at or below concentrations the compounds normally exhibit anti-parasitic activity. Thiazolides induced typical signs of apoptosis, such as nuclear condensation, DNA fragmentation and phosphatidylserine exposure. Interestingly, the apoptosis-inducing effect of thiazolides appeared to be cell cycle-dependent and induction of cell cycle arrest substantially inhibited the cell death-inducing activity of these compounds. Using affinity chromatography and mass spectrometry glutathione-*S*-transferase P1 (GSTP1) from the GST class Pi was identified as a major thiazolide-binding protein. GSTP1 expression was more than 10 times higher in the thiazolide-sensitive Caco2 cells than in the less sensitive HFF cells. The enzymatic activity of recombinant GSTP1 was strongly inhibited by thiazolides. Silencing of GSTP1 using siRNA rendered cells insensitive to RM4819, while overexpression of GSTP1 increased sensitivity to RM4819-induced cell death. Thiazolides may thus represent an interesting novel class of future cancer therapeutics.

Key words: apoptosis; colon cancer; cell cycle; oncogene

Thiazolides are a novel class of anti-infective agents with potent activity against a wide variety of helminths, protozoan parasites, anaerobic bacteria and viruses.[1,2] The thiazolides are derived from nitazoxanide (NTZ [2-acetolyloxy-*N*-(5-nitro 2-thiazolyl) benzamide]), which was originally developed as a veterinary anthelminthic.[3] Subsequently, the drug has been shown to exhibit a broad spectrum of activity *in vitro* and *in vivo* against parasites such as *Entamoeba histolytica*,[4] *Giardia lamblia*,[4–6] *Cryptosporidium parvum* and *Sarcocystis neurona*,[7–10] and a range of anaerobic bacteria infecting animals and humans,[1,2,8,10] and viruses.[11] *In vitro* activities of NTZ and other thiazolides have been demonstrated against intracellular pathogens such as the apicomplexan parasites *Neospora caninum, Toxoplasma gondii*[12–14] and *Besnoitia besnoitii*.[15]

Following oral uptake *in vivo*, NTZ is rapidly deacetylated to tizoxanide (TIZ),[16] a compound with equal effectiveness.[4,6] In the liver, TIZ is then transformed to tizoxanide glucuronide (TIG) and excreted *via* bile or urine.[16] NTZ and TIZ are considered to have low toxicity for mammals and to have few side effects. There is, however, only a relatively small amount of data to support this.[2]

Further, the anti-parasitic activities of nitro- and non-nitro thiazolides differ considerably with respect to intracellular and extracellular parasites: in the intracellular apicomplexan *N. caninum* cultured in HFF and other mammalian cells, not only nitro-thiazolides such as NTZ and TIZ, but also thiazolides with a bromo- instead of a nitro group, exhibit considerable activity.[12–14] These drugs appear to interfere in parasites proliferation by inducing egress and preventing subsequent host cell invasion, and these effects were found to be, at least partially, mediated by the host cells.[12–14] In contrast, in axenically cultured *G. lamblia*, the thiazole-associated nitro group is a prerequisite for efficient antigiardial activity, and bromo- and carboxy-thiazolides have proven to be rather ineffective in axenic cultures.[6] The molecular mechanism of thiazolides in the infectious agent is largely unknown but direct effects on host cells such as Caco2 have been observed (Müller, unpublished data). Thus, some of the thiazolide effects on parasites could be mediated by the host cells.

There is little information on possible molecular targets for NTZ and other thiazolides. However, the current evidence clearly indicates that the mechanisms of action are different in extracellular versus intracellular pathogens.[2] Pyruvate oxidoreductase (POR) has been described as a major target of NTZ in extracellular pathogens by showing that NTZ inhibits POR enzyme activity from H. pylori and other anaerobes *in vitro*.[17,18] In addition, other potential targets could be involved. Affinity chromatography employing TIZ covalently linked to agarose has recently been used to identify a *G. lamblia* nitroreductase (GlNR1) as a major TIZ-binding protein and enzyme activity assays employing recombinant GlNR1 confirm its role as a potential NTZ-target.[19] In the intracellular parasite *N. caninum*, a protein disulfide isomerase (NcPDI) has been identified as a putative target.[20] The enzyme activities of NcPDI[20] and of 2 PDIs from *G. lamblia*[21] are inhibited by NTZ and other thiazolides *in vitro*.

In this study we present the direct effects of thiazolide treatments on uninfected HFF and Caco2 cells, and show that thiazolides, and most notably RM4819, severely impair Caco2 cell proliferation and structural integrity, but affect HFF-proliferation to a much lesser extent. RM4819-agarose affinity chromatography identified glutathione-*S*-transferase GSTP1 from the GST class Pi, one of the 7 classes (Alpha, Mu, Pi, Theta, Sigma, Zeta, Omega) of mammalian cytosolic GSTs,[22–24] as a major Caco2 cell thiazolide-binding protein. GSTPis are overexpressed in various malignant tumors such as colon cancer and lung cancer, and are considered to increase chemoresistance by inactivating of chemotherapeutics through coupling to glutathione.[24] We show that thiazolides impair the enzymatic activity of GSTP1 and that GSTP1 expression and the impact of thiazolides is much stronger in Caco2 cells than in HFF cells. Furthermore, we demonstrate that thiazolide activity in Caco2 and HFF cells is cell cycle-dependent. Using RNA interference, we show that knock-down of GSTP1 reduces sensitivity of Caco2 cells to RM4819. These data indicate that GSTP1 is an important target of thiazolide-induced apoptosis in cancer cells.

Joachim Müller and Daniel Sidler contributed equally to this work.

Grant sponsors: Stanley Thomas Johnson Foundation; Oncosuisse; University of Berne; Swiss National Science Foundation; Grant number: 3100A0-112532/1.

***Correspondence to:** Institute of Parasitology, University of Berne, Länggass-Strasse 122, CH-3012 Berne, Switzerland.
Fax: +41-31-6312477. E-mail: hemphill@ipa.unibe.ch

Material and methods

Tissue culture media, biochemicals and drugs

If not stated otherwise, all biochemical reagents were from Sigma (St. Louis, MO). The thiazolides (see Table I) were synthesized at the Department of Chemistry, University of Liverpool or at the Department of Biochemistry and Chemistry, University of Berne. They were kept as 100 mM stock solutions in DMSO at −20°C.

Cell culture

The human colon cancer cell line Caco2 (ATTC HTB-37) and Human Foreskin Fibroblasts (HFF) were kindly provided by Erwin Sterchi and Daniel Lottaz, Institute of Biochemistry and Molecular Biology, University of Bern. Human embryonic kidney fibroblasts 293T cells were obtained from the American Type Culture Collection (Manassas, VA). Cells were cultured in Dulbecco's modified Eagle's medium containing 10% fetal calf serum, 50 U/ml of penicillin, and 50 μg/ml of streptomycin (Caco2 growth medium) at 37°C and 5% CO_2.

Drug efficacy assays

For determining effects of thiazolides on cell proliferation, cells were trypsinized, suspended in fresh medium, and transferred to 24-well-plates (5×10^3 cells per well) containing the drugs (0–50 μM) or DMSO as a solvent control. After 72 h, the medium was removed, attached cells were washed with PBS, trypsinized and counted using a Neubauer chamber.

Electron microscopy

For transmission (TEM) electron microscopy, Caco2 cells were treated with doxorubicine (2 μM), RM4819 (25 μM) or with DMSO as solvent control for 6, 12, and 24 h, respectively, and treated cells were harvested as described above and resuspended in 1-ml ice cold PBS, transferred to 1.5-ml Eppendorf tubes and centrifuged (2,300*g*, 5 min, 4°C). Pellets were resuspended in 100 mM cacodylate pH 7.3 containing 2.5% glutaraldehyde and fixed overnight at 4°C. Pellets were then washed 3 times in 100 mM cacodylate buffer, and postfixed in 100 mM cacodylate containing 1% OsO_4 for 2 h. Pellets were then washed 3 times in distilled water and contrasted in saturated uranyle acetate for 30 min and dehydrated in ethanol series (50, 70, 90%, 3× 100%). Pellets were embedded in Epon 820 resin, and the resin was polymerized at 65°C over a period of 48 h. Ultrathin sections were cut on a Reichert and Jung ultramicrotome and were loaded onto 300 mesh copper grids (Plano GmbH, Marburg, Germany). Staining with uranyle acetate and lead citrate was performed as described. Finally, grids were viewed on a Phillips CM12 transmission electron microscope operating at 80 kV.[25]

TABLE I – OVERVIEW OF COMPOUNDS MENTIONED IN THIS STUDY

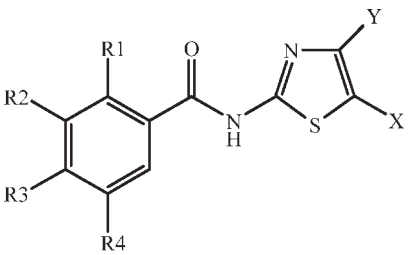

Compound	X	R1	R2
NTZ	NO_2	$OCOCH_3$	H
TIZ	NO_2	OH	H
TIG	NO_2	O-Glucuron	H
RM4819	Br	OH	CH_3
RM4825	COOH	OH	H

The numeration is indicated on the generic thiazolide formula. In the compounds studied, R3, R4, and Y were H.

Annexin-V staining

Annexin-V staining was performed as described previously.[26] Cells were analyzed using flow cytometry (FACScan, BD) and data analyzed using the FlowJo software package (Ashland, OR).

MTT assay

Cell viability was measured by using the MTT assay, as described previously.[27] Briefly, cells were cultured in 96-well plates and challenged with compounds or DMSO controls for 40 h. Then, plates were centrifuged (1,000*g*, 5 min, 4°C), culture medium was discarded and replaced with 0.5 mg/ml MTT (3-(4,5-Dimethylthiazol-2-yl)-2,5-diphenyltetrazolium bromide) in culture medium for 3 hr. Plates were again centrifuged, medium was discarded and replaced by DMSO to dissolve the formazan. Absorbance was measured at 570 nm using a microplate reader (SpectraMAX, Molecular Devices, Sunnyvale, USA). Cell viability was expressed as a percentage of the value in control cultures.

Cell cycle analysis

Cell cycle analysis was performed as follows. Cells were cultured in 24-well-plates and stimulated with compounds or DMSO control for 40 h. Then, cells were collected and washed in PBS, followed by incubation with hypotonic propidium iodide solution (200 μg/l propidium iodide in 0.5× PBS, 0.1% Triton-X100) for 30 min on ice. DNA staining was analyzed by flow cytometry and cell cycle profiles were evaluated using the FlowJo software package. In some experiments, cell cycle was inhibited by treatment with nocodazole (150 ng/ml), 12 h prior to treatment with compounds or DMSO controls.

Protein extraction

Caco2 cells were grown in 175 cm^2-culture flasks, trypsinized, transferred to 50-ml-Falcon tubes and pelleted (1,000*g*, 10 min, 4°C). Pellets were transferred to Eppendorf tubes, washed 3 times with PBS followed by centrifugation (2,300*g*, 6 min, 4°C) and stored at −20°C. For protein extraction, frozen pellets corresponding to about 5×10^7 Caco 2 cells were resuspended in ice cold extraction buffer, *i.e.*, PBS containing 1% Triton-X-100 and 1 mM phenyl-methyl-sulfonyl-fluoride. Suspensions were vortexed thoroughly, and centrifuged (15,200*g*), 10 min, 4°C). Extraction of pellets was repeated twice. For 5×10^7 cells, 5 ml of extraction buffer were used in total. Supernatants were combined (5–10 mg of total protein) and subjected to RM4819-agarose affinity chromatography.[19]

Affinity chromatography using RM4819-agarose

To produce RM4819-agarose, 0.7 g lyophilized epoxy-agarose with a C-12-spacer was suspended in 15 ml H_2O and centrifuged at 300*g* for 5 min. Washes in water were repeated twice, and once using coupling buffer ($NaHCO_3$ 0.1 M, pH 9.5). After the last wash, epoxy-agarose was suspended in 2.5 ml coupling buffer. About 20 mg RM4819 were dissolved in 2.5 ml dimethyl-formamide and added to the agarose. The mixture was incubated for 3 days at 37°C under slow but continuous shaking to allow coupling of the epoxy group to RM4819 *via* the OH— group in Position 2 of the C6-ring (see Table I). The resulting column medium (∼2 ml) was then transferred to a chromatography column (Novagen, Merck, Darmstadt, Germany) and the column was washed with coupling buffer (20 ml). This was followed by ethanolamine (1 M, pH 9.5) for 4 h at 20°C in the absence of light to block residual reactive groups. Finally, the column was extensively washed with PBS and PBS/DMSO (1:1) to remove unbound RM4819. The RM4819 column was stored in PBS containing 0.02% NaN_3 at 4°C.

Prior to affinity chromatography, the column was washed with 50 ml PBS equilibrated at 20°C. Crude extracts (5 ml) prepared as

TABLE II – OVERVIEW OF PRIMERS USED IN THIS STUDY

Gene	Accession number	Region of CDS	Primer (5′|3′)
GSTP1	CAA30894	CDS 1–630	GSTP1F CACCCCGCCCTACACCGTGGTC
			GSTP1R CTCACTGTTTCCCGTTGCCA
			HGSTP1MF AAGCTTCGATGCCGCCCTACACCGTG
			HGSTP1MR GGATCCGACTGTTTCCCGTTGCCATTGA
		CDS 1–221	GSTPquantF ATGCCGCCCTACACCGTG
			GSTPquantR CCAGGTGACGCAGGATGG
Actin	NM_001100	CDS 761–893	α-AC1 GAGACCACCTACAACAGCATCATG
			α- AC2 CACCTTGATCTTCATGGTGCTGGG

CDS = coding sequence.

described above were loaded with a flow rate of about 0.25 ml/min. The column was washed with PBS until the baseline was flat (8 column volumes, corresponding to about 24 ml). Proteins binding to the column were eluted with 1 mM NTZ in PBS followed by elution with a pH shift (Glycine Cl^- 100 mM, pH 2.9) to remove nonspecifically-bound proteins. Moreover, fractions were taken before elution with NTZ (pre-NTZ) or pH shift (pre-pH shift). Sizes of these fractions ranged between 3 and 5 ml. From all fractions, 0.05- to 0.2-ml aliquots were taken for analysis by SDS PAGE. SDS-PAGE was performed according to Laemmli[28] using a Hoefer Minigel 250 apparatus (Amersham, GE Healthcare, Little Chalfont, United Kingdom). Silver staining was performed according to Blum *et al.*[29]

Protein sequencing by mass spectrometry

For protein sequencing, the NTZ eluates with the highest amounts of binding protein were pooled and dialyzed against ammonium bicarbonate (1 g/l) for 4 h, then against 0.4 g/l overnight at 4°C in the dark. The dialyzed fraction was then lyophilized. Aliquots of the lyophilized binding protein (ca. 200 ng) were suspended in SDS-PAGE sample buffer, loaded on a 12% acrylamide gel and subjected to electrophoresis. After staining with colloidal coomassie (0.1% Coomassie Brilliant Blue G 250 in 34% MeOH with 0.5% acetic acid and 17% ammonium sulfate), a band of about 25 kDa was excised and processed for mass spectrometry analysis and performed as described.[19]

Cloning and heterologous expression of GSTP1 in E. coli

To clone GSTP1 into the His-tag-expression vector pET151 directional TOPO (Invitrogen, Carlsbad, CA), the primers pGSTPfor and pGSTPrev (Table II) were created for the amplification of a 634 base pair product encoding the GSTP1 (CAA30894) polypeptide with 4 additional bases at the 5′ end allowing directional cloning (MWG Biotech, Ebersberg, Germany) as previously described.[19,21] For amplification by PCR, RNA was extracted from 5×10^6 Caco2 cells using the Qiagen RNeasy including a DNase I digestion (to remove residual genomic DNA) kit according to the instructions provided by the manufacturer. RNA was eluted with 50 µl RNase-free water and stored at −80°C.

First strand cDNA was synthesized using the Qiagen OmniscriptRT kit as described by the manufacturer. The PCR reaction was performed using 0.6 µ pfu (Promega, Madison, WI), 2 µl pfu buffer 10× (Promega), 20 pmol of each primer, 0.16 mM dNTPs (Promega) on 0.5 µl of cDNA diluted 1/10 in a total volume of 20 µl. The annealing temperature was 62°C. The resulting 634 bp-product was inserted into pET151 vector using the respective cloning kit according to the manufacturer, and the vector was transformed into *E. coli* TOP 10 cells (Invitrogen). Heterologous expression of GSTP1 in *E. coli* and His-tag purification was performed as described.[19]

Overexpression of pEGFP-GSTP1 in 293T cells

Full length cDNA of GSTP1 was amplified using the primers HGSTPiMF and R, which resulted in a 634 bp product. The PCR product was ligated into the Zero blunt TOPO cloning vector as described by the manufacturer (Invitrogen, Carlsbad, CA). The insert was cleaved by HindIII and BamH1 (Promega, Madison, WI) and subcloned into pEGFP-C1.

For overexpression studies, HEK 293T cells were seeded in 6-well plates and transfected with pEGFP-GSTPi or pEGFP as control vector using the calcium phosphate transfection method. After 16 h, cells were trypsinized and seeded in 96-well plates and challenged with thiazolides RM4819 and RM4825 (0–20 µM) for 40 h. Then cell viability was determined using MTT.

GST enzyme assay

GST activity was measured by a photometric assay based on the coupling of glutathione to chloro-dinitrobenzene.[30,31] The assay was performed in 96-well microtiter plates (Nunc) with 174 µl assay buffer (PBS, pH 7.2) per well containing 0.5 mM chloro-dinitrobenzene (100 mM stocks in DMSO) and recGSTP1 (0.5 µl) or buffer (enzyme blank). The reaction was started by addition of 6 µl glutathione (30 mM in PBS; 1 mM as final concentration). After 5-min preincubation, absorbance at 340 nm was read at various time points (0–20 min) on a 96-well-plate spectrophotometer (Versamax, Molecular Devices, Sunnyvale CA). Enzyme activity was calculated from the linear increase of absorption over time.

Quantification of GSTP1 expression in Caco2 cells and HFF by real-time RT-PCR

Caco2 and HFF cells were harvested and RNA was extracted using the Qiagen RNeasy kit (Qiagen Haiden, D). RNA was eluted with 50 µl RNase-free water and stored at −80°C. First strand cDNA was synthesized using the Qiagen OmniscriptRT kit as described by the manufacturer. The primers GSTP1quantF and GSTP1quant R (Table II) were used for the quantification of GSTP1 expression. Quantitative PCR was performed as described with the annealing temperatures 60°C for GSTP1 and 55°C for actin. From the quantitative RT-PCR, mean values (±SE) from triplicate determinations were assessed and expression levels were given as values in arbitrary units relative to the amount of actin RNA.

RNA interference

CaCo2 cells were plated in 6-well plates and let to adhere. Then, cells were transfected with 10 nM siGSTPi (Dharmacon ON-TARGET plus SMARTpool, human GSTP1, L-011179-00-0005, Thermo Fisher Scientific, Lafayette, CO) using Hyperfect transfection reagents (Qiagen) for 24 h. The efficacy of GSTPi knockdown was analyzed after 24 h by realtime RT-PCR as described above. Cells were trypsinized and seeded in 96-well plates challenged with the thiazolides RM4819 and RM4825 (0–20 µM), or doxorubicine (0.2 µM) for 40 h. Cell viability was measured by MTT.

Statistics

IC_{50} values were calculated after to the logit-log-transformation of the relative growth (RG; control = 1) according to the formula $\ln[(RG/(1 - RG)] = a \times \ln(\text{drug concentration}) + b$ and subsequent regression analysis by the corresponding software tool contained in the Excel software package (Microsoft, Seattle, WA).

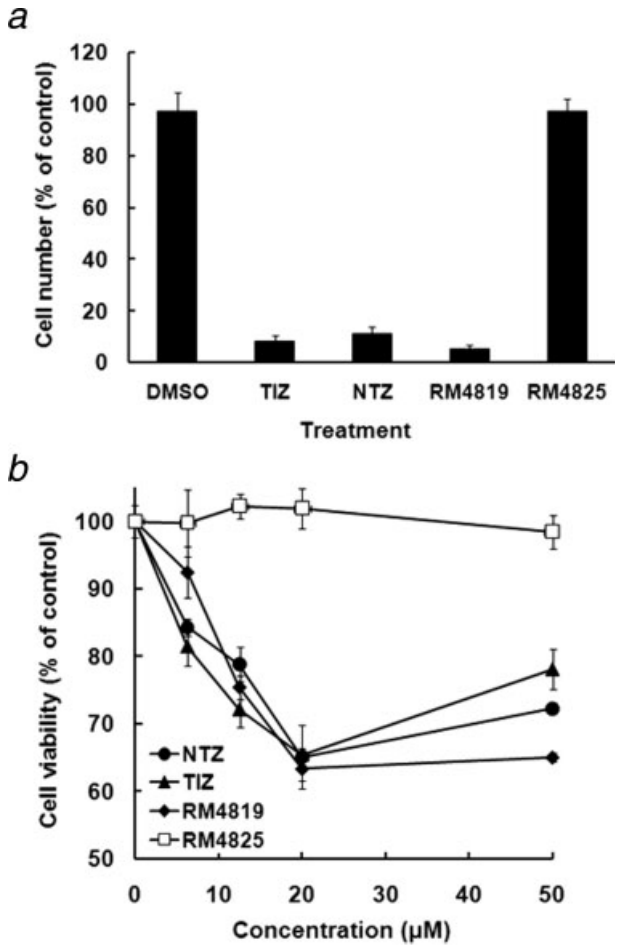

Figure 1 – Effects of thiazolides on growth of Caco2 cells. (*a*) 5×10^3 cells per well were seeded to 24-well-plates together with the thiazolides NTZ, TIZ, RM4819, RM4825 (50 μM) or DMSO as a solvent control. After 72 h, cells were harvested by trypsinization and counted. Mean values (±SE) are given in percentage of the mean control value for quadruplicates. (*b*) 10^3 Cells per well were seeded to 96-well-plates. After 48 h, medium was replaced by fresh medium containing the thiazolides NTZ, TIZ, RM4819, RM4825 (0 to 50 μM) or DMSO as a solvent control. After 40 h, cell viability was assayed using MTT. Mean values (±SE) are given in percentage of the mean control value for triplicates.

Analysis of variance and subsequent pair-wise *t* tests were performed using the Excel software package (Microsoft, Seattle, WA).

Results

Effects of thiazolides on HFF and Caco2 cells

To investigate effects of thiazolides on human cells, growth experiments were performed with Caco2 cells in the presence of the nitro-thiazolides TIZ and NTZ, the bromo-thiazolide RM4819 and the carboxy-thiazolide RM4825. At a concentration of 50 μM, NTZ, TIZ, and especially RM4819 strongly depressed Caco2 cell number whereas RM4825 was ineffective (Fig. 1*a*). The results were similar when cell viability was determined using an MTT assay after 40 h instead of 72 h (Fig. 1*b*). To investigate this in more detail, concentration series with the most active compound, RM4819, and RM4825 and DMSO as controls, were performed and effects on Caco2 cells were investigated (Fig. 2*a*). Addition of increasing concentrations of RM4819 to Caco2 cells resulted in a strongly decreased number of cells recovered after 72 h, with an

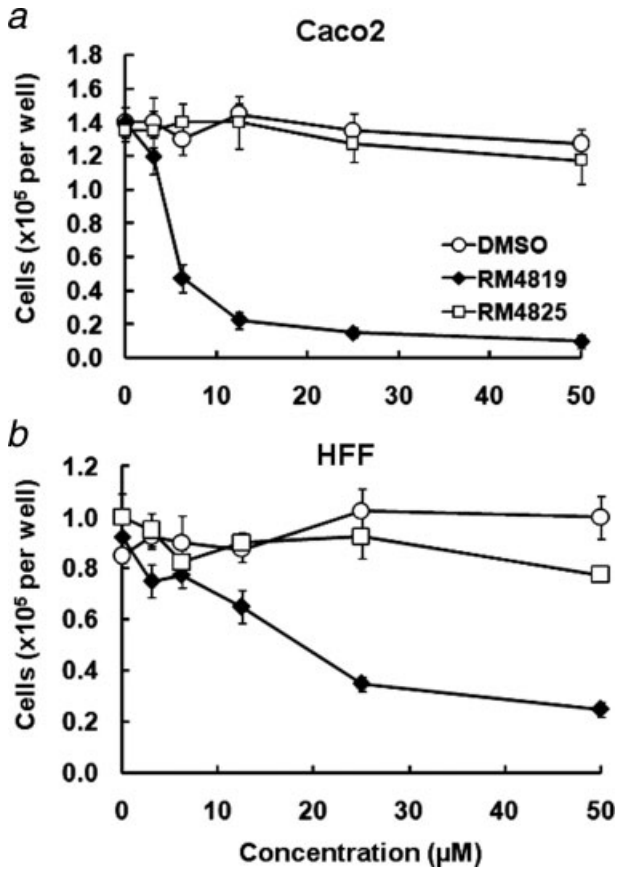

Figure 2 – Effects of thiazolides on Caco2 and HFF cells. To determine effects on proliferation, 5×10^3 cells were seeded to 24-well-plates together with the thiazolides RM4819, RM4825 (0–50 μM) or DMSO as a solvent control. After 72 h, cells were harvested by trypsinization and counted. Mean values (±SE) are given in percentage of the mean control value for quadruplicates. (*a*) Caco2 cells; (*b*) HFF cells.

IC_{50} value of 6.8 ± 1.3 μM (Fig. 2*a*). HFF, representing nontransformed cells, were much less susceptible when subjected to the same type of experiment, and cell number was decreased only at much higher concentrations of RM4819 (IC_{50} 18.9 ± 1.2 μM) (Fig. 2*b*). Besides Caco2 cells, 2 other colon carcinoma lines, such as T84 and HT29, were found to be sensitive to TIZ and RM4819, but not to RM4825 (data not shown).

The thiazolide RM4819 induces apoptosis

To investigate whether reduced cell proliferation was due to cell death induction rather than inhibition of proliferation, Caco2 cells were treated with RM4819 and the chemotherapeutic drug doxorubicine as a positive control, and ultrastructures of cells were examined by TEM. In control-treated cultures (Fig. 3*a*), Caco2 cells had formed confluent layers with a defined cellular polarity. Microvilli-like structures were clearly visible at the apical part of the cell surface, and typical epithelial-like cell–cell contacts such as tight junctions were formed. At 6 h of treatment with RM4819, alterations were observed in about 50% of the cells, such as partial loss of microvilli at the apical surface and increased cytoplasmic vacuolization (Figs. 3*b* and 3*c*). However, intact and altered cells were observed sitting side-by-side, and were still connected by cell–cell junction structures (Fig. 3*c*). At 12 h of treatment with RM4819 (Fig. 3*d*), the destructive effects of the drug became more evident, as illustrated by the complete loss of microvilli organization in most of the cells, and the formation of small and large cytoplasmic vacuoles, often filled with electron dense

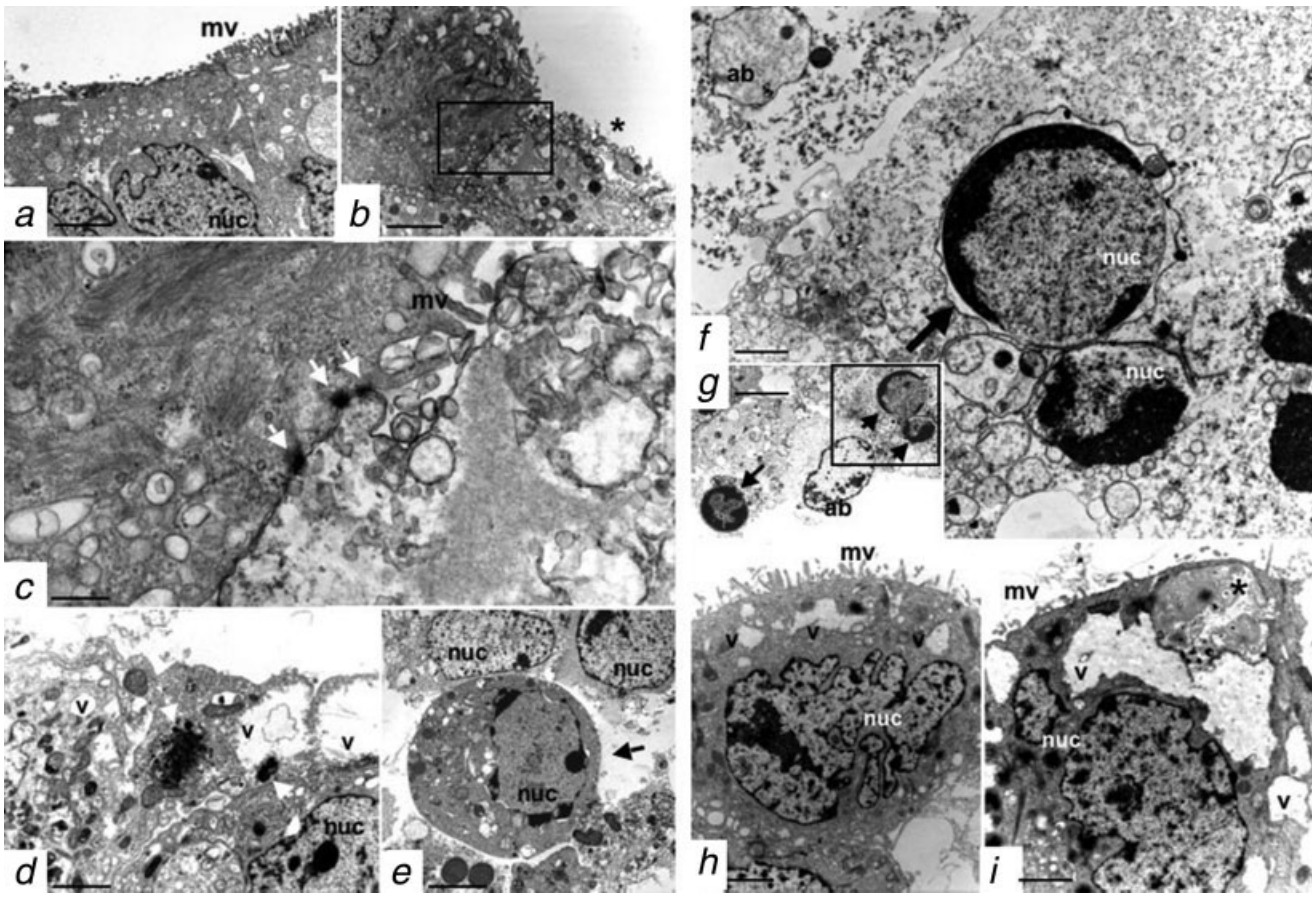

Figure 3 – TEM of Caco2 cell cultures exposed to RM4819 (25 μM) for 0–12 h. (*a*) low magnification overview of control Caco2 cells exhibiting a polarized organization. Microvilli in the apical portion are depicted with mv; bar = 10 μm. (*b*) (low magnification) and (*c*) (high magnification), Caco2 cells treated with 30 μM Rm4819 for 6 h. A cell showing alterations in (*b*) is marked with a * just adjacent and connected through tight junctions (arrows in *c*) to a largely unaltered cell with still intact microvilli (mv). Bar in *b* = 10 μm, in *c* = 2 μm. (*d*) Low magnification TEM view of cells treated with RM4819 for 12 h. Increasing occurrence of alterations such as loss of microvilli and increased cytoplasmic vacuolisation (v) is evident. Arrows point towards electron dense cytoplasmic inclusions. Bar = 10 μm). (*e*) Low magnification TEM view of cells treated with RM4819 for 24 h. Arrow points towards rounded-up Caco2 cell displaying typical sign of apoptosis including chromatin condensation most notably at the periphery of the nucleus. Bar = 50 μm. (*f–i*) TEM of Caco2 cell cultures exposed to RM4819 (25 μM) and doxorubicin (2 μM) for 24 h. (*f*) High magnification (bar = 5 μm) and (*g*) corresponding low magnification view (bar = 20 μm) of apoptotic features of Caco2 cells treated with RM4819 for 24 h. ab = apoptotic bodies, arrows point towards nuclei exhibiting extensive chromatin condensation. (*h* and *i*) show doxorubicin-treated Caco2 cells, exhibiting extensive cytoplasmic vacuolization, nuclear fragmentation and partial chromatin condensation (nuc), and intracytoplasmic membrane stacks are depicted by an asterisk (*). Bars = 5 μm.

material. At 24 h, the RM4819-treated cells had lost polarization, rounded up and exhibited extensive chromatin condensation, disintegration of cytoplasmic organization, and the formation of structures resembling apoptotic bodies (Figs. 3*e*–3*g*). Cells treated with doxorubicine exhibited distinct properties of cells undergoing apoptosis such as vacuolization of the cytoplasm, fragmentation of the nucleus, and the presence of intracytoplasmic membrane stacks (Figs. 3*h* and 3*i*). These data suggest that treatment of Caco2 cells with RM4819 leads to cellular alterations typically associated with apoptotic cell death.

RM4819 induces phosphatidylserine exposure and DNA fragmentation

To see whether, besides these ultrastructural alterations, other markers for apoptosis were found, Caco2 cells were treated with RM4819, RM4825, doxorubicine or DMSO as a negative control. After 24 h, cells were harvested, and phosphatidylserine exposure was detected by Annexin V-staining. Cells treated with RM4819 and doxorubicine were to more than 60% Annexin-V-positive. These differences were highly significant (ANOVA, $p < 0.01$) whereas cells treated with RM4825 were at control levels (ANOVA, $p > 0.1$; Fig. 4*a*). Furthermore we assessed whether RM4819 induced DNA fragmentation, typically associated with apoptotic cell death. Figure 4*b* illustrates that both RM4819 and doxorubicine treatment resulted in a higher frequency of cells with a sub-G1 (fragmented) DNA content. In contrast, RM4825-treated cells had similar levels of DNA fragmentation as control treated cells. Notably, doxorubicine but not RM4819 induced a cell cycle arrest. Thus, we conclude that RM4819 induces apoptosis rather than cell cycle arrest in Caco2 cells.

RM4819 acts primarily on proliferating cells

Various chemotherapeutic drugs induce cell death in a cycle-dependent manner, *i.e.*, by inducing DNA damage and activating tumor suppressor genes. To assess cell cycle dependency, Caco2 and HFF cells were grown to confluency and RM4819-induced cell death was analyzed. Interestingly, confluent HFF were resistant to RM4819 treatment, whereas Caco2 cells remained sensitive (data not shown). In contrast to HFF, Caco2 cells do not show contact-dependent cell cycle arrest. Caco2 cells were thus treated with the cell cycle inhibitor nococdazole, which resulted in a substantial inhibition of cell cycle progression and an arrest in G2/M

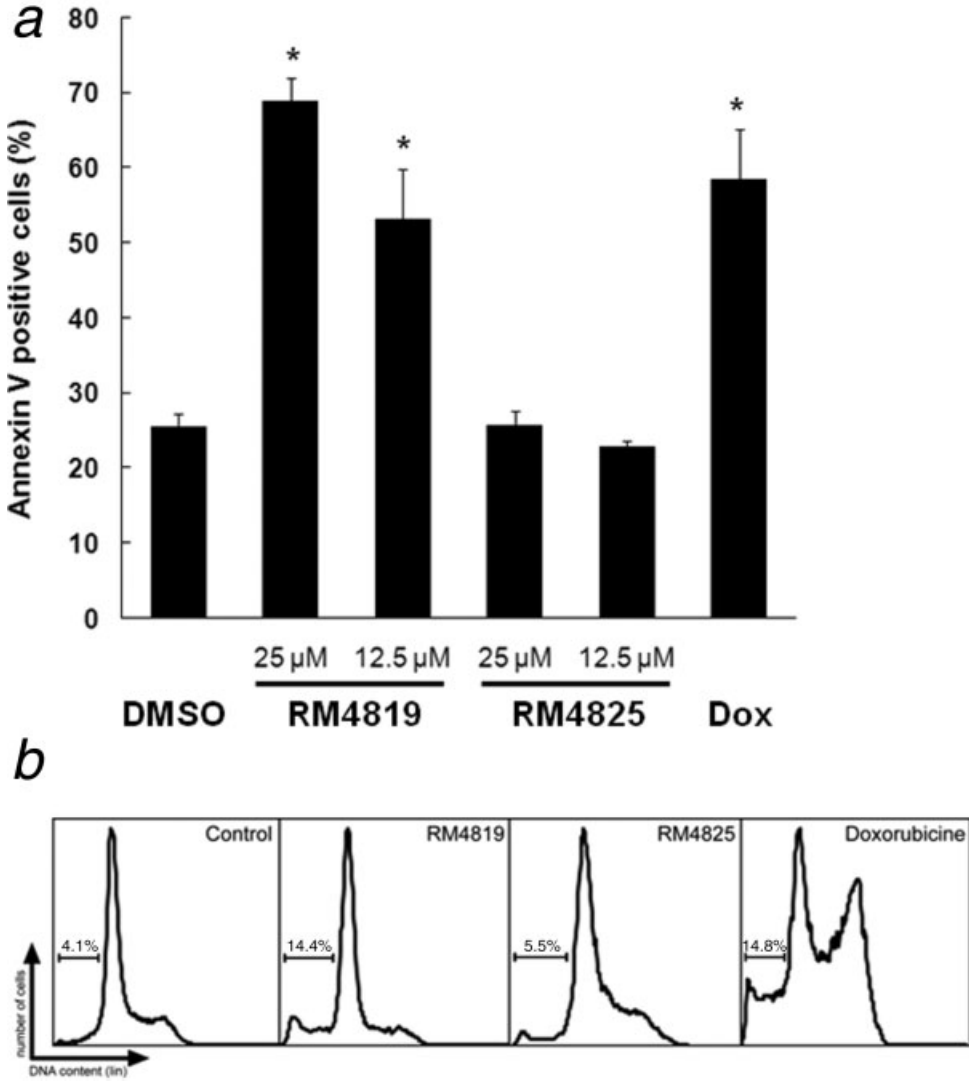

Figure 4 – (*a*) Caco2 cells treated with RM4819 become annexin-V-positive. Caco2 cells were grown in 24-well-plates. After 48 h, medium was replaced with fresh medium containing the thiazolides RM4819, RM4825 (12, 5, 25 µM), doxorubicine (Dox, 4.6 µM) or DMSO as a solvent control. Cells were harvested and stained for annexin-V after 24 h. Assays were run in triplicate. Mean values (±SE) are given. Values superscribed by asterisks (*) are significantly different from DMSO controls (ANOVA followed by pairwise t-tests, $p < 0.01$). (*b*) RM4819 induces DNA fragmentation. Caco2 cells were grown in 24-well plates and stimulated with RM4819, RM4825 (25 µM), doxorubicine (2 µM) or DMSO as a solvent control for 40 hr. Then, cells were stained with propidium iodide for 30 min on ice. DNA staining was analyzed by flow cytometry and cell cycle profiles were evaluated using the FlowJo software package. The sub-G1 (fragmented) DNA content is given.

(Fig. 5*a*). Control cells and cell cycle arrested cells were then treated with RM4819 or RM4825, and cell viability was measured by MTT assay. Remarkably, only control treated Caco2 cells were susceptible to RM4819, whereas cells treated with nocodazole (Fig. 5*b*) were substantially protected from RM4819-induced cell death. Nocodazole had neither alone nor in combination with RM4825 had an effect on Caco2 viability. These data indicate that RM4819 acts only on actively proliferating cells.

GSTP1 is the major RM4819-binding protein

Since the thiazolide RM4819 was found to be the most active compound in Caco2 growth inhibition experiments (see Fig. 1), we aimed at identifying the cellular target of this compound. RM4819 coupled to epoxy-agarose and following RM4819-affinity chromatography of Caco2 cytoplasmic extracts, a major protein of ~25 kDa was eluted with 1 mM NTZ (Fig. 6*a*). The 25-kDa protein was subjected to mass spectrometry analysis. Nine peptides aligned with a high probability to the human glutathione-*S*-transferase (GST) P1 (E.C.2.5.1.18; accession protein CAA30894; cDNA X06547), a GST from class Pi (Fig. 6*b*). Performance of RM4819-affinity chromatography with HFF extracts under the same conditions did not yield any RM4819-binding proteins, indicating that either no such proteins were synthesized in HFF, or that expression of potential binding proteins, such as GSTP1, was diminished in nontransformed cells compared to colon cancer cells. Indeed we found that Caco2 cells had several fold higher levels of GSTPi mRNA than HFF cells (Fig. 6*c*).

*The glutathione-*S*-transferase activity of recombinant GSTP1 (recGSTP1) is inhibited by thiazolides*

To test whether thiazolides would inhibit the enzymatic activity of GSTP1, the human GSTP1 cDNA was cloned and expressed in *E. coli* as an N-terminally His-tagged recombinant protein (recGSTP1), and recGSTP1 was purified by Ni^{2+}-affinity chroma-

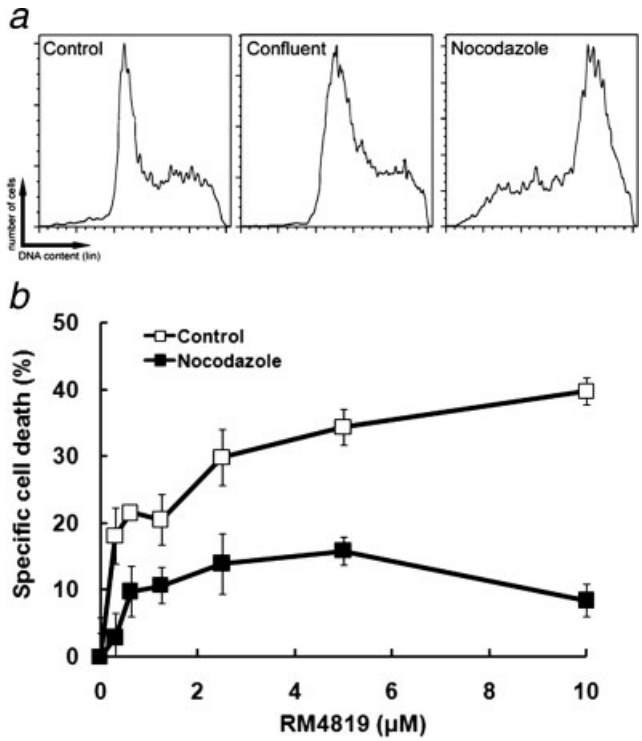

Figure 5 – RM4819 affects viability of proliferating cells only. (*a*) CaCo2 cells plated in 6 (A) or 96 well plate (*b*) and let to adhere. Cells were treated with the cell cycle inhibitor nocodazole (150 ng/ml) or DMSO as a solvent control for 12 h. Then samples were taken for cell cycle analysis by flow cytometry (*a*) or challenged with the thiazolides RM4819 or RM4825 for 40 h. Specific cell death as compared to untreated controls was determined by MTT assay (*b*). ssays were run in triplicate. Mean values (±SE) are given.

tography (Fig. 7*a*). The purified protein had a size of ~30 kDa due to N-terminal, vector-born sequences. RecGSTP1 was enzymatically active as measured by the coupling of glutathione to chloro-dinitrobenzene. In agreement with the cell death-inducing activity of thiazolides and their specific binding to GSTP1, the enzymatic activity of recGSTP1 was efficiently inhibited by TIZ and RM4819, but not by RM4825, in a concentration-dependent manner (Fig. 7*b*). At a substrate concentration of 0.5 mM chloro-dinitrobenzene, 50% inhibition were achieved with 11.4 ± 1.3 μM RM4819 and with 14.8 ± 1.2 μM TIZ. Other bromo- and nitro-thiazolides inhibited recGSTP1 to similar extents (data not shown). Assuming a competitive interaction with chloro-dinitrobenzene and a K_m for chloro-dinitrobenzene of 0.98 mM,[30] a K_i value of 4.5 ± 1.2 μM was calculated for RM4819 and 6.8 ± 1.6 μM for TIZ.[32]

Alteration of GSTP1 expression affects sensitivity to RM4819

To investigate, whether expression levels of GSTPi affect the sensitivity to RM4819, overexpression or knockdown of GSTPi were performed in Caco2 cells. Silencing of GSTP1 with siRNA led to a decrease of GSTP1 mRNA levels to less than 25% of the control levels within 24 h (Fig. 8*a*). This decrease was still maintained after 48 h (data not shown) and correlated with a significantly lower sensitivity to RM4819 in silenced Caco2 cells as compared to control cells. Conversely, GSTP1 knockdown cells exhibited a higher susceptibility to doxorubicine (Fig. 8*b*). Overexpression of GSTPi-GFP was performed in HEK293T cells due to the very high transfection efficacy (data not shown). After 24 h, GSTP1 mRNA levels reached more than 100 times the value of control transfected 293T cells and more than 10 times the levels of control Caco2 cells (Fig 8*a*). Interestingly, sensitivity of HEK 293T cell significantly increased after GSTPi overexpression compared to control transfected cells, in particular at low RM4819 concentrations (Fig. 8*c*).

Discussion

Our study shows that several thiazolides, namely NTZ, TIZ, and, especially, the bromothiazolide RM4819, are not only effective against bacteria, protozoa or helminths, but also against proliferating human cells in a comparable micromolar concentration range. These results are relevant in the light of the fact that NTZ is currently marketed for use against cryptosporidiosis and giardiasis in adults.[1,10] Although there are reports on mild to moderate side effects of NTZ application,[1,2,10] the potential nature of effects of NTZ and other thiazolides like RM4819 in cultured human cells has never been reported.

The efficacy of RM4819 is much more pronounced in rapidly proliferating cells such as the colon cancer cell line Caco2 and other colon carcinoma lines such as T84 and HT29 (data not shown). If proliferation is inhibited by treatments with nocodazole, a substantially less RM4819-mediated cell death induction was observed. RM4819 also acts against proliferating nontransformed HFF (albeit at a three times higher IC_{50}), but does not show any affect in confluent, nonproliferating HFF monolayers. Thus, these data clearly indicate that cell cycle progression is a prerequisite for thiazolide-induced cell death.

The drug-treated Caco2 cells exhibited typical features reminiscent of apoptotic cells, such as nuclear condensation, phosphatidylserine exposure and DNA fragmentation. This suggests that RM4819 can activate the cellular apoptosis machinery. However, more detailed investigations are necessary to clarify how these drugs induce cell death in colon carcinoma cells. Nevertheless, the property of these thiazolides to induce cell death in rapidly dividing cells more efficiently than in quiescent confluent cells mirrors the capacity of thiazolides to act on rapidly replicating parasites.

Affinity chromatography employing immobilized drugs is one of several approaches that can be used to identify drug–proteins interactions. Using RM4819-agarose affinity chromatography, human GSTP1 was isolated and identified as a major thiazolide-binding protein. In addition, several thiazolides inhibited the enzymatic activity of recGSTP1 in a concentration that also inhibited growth of Caco2 cells. GSTP1, a member of the GST class Pi,[23] is a homo-dimer (GSTP1-1) normally found in the placenta. It has been extensively studied since it is expressed at high levels in many malignant tumors.[24] The GSTP1 gene is located on chromosome 11q13 in a region where other cancer-associated genes and oncogenes are found.[30] Several isoforms are known differing in substitutions in amino acid 104 (I to V) or amino acid 113. These isoforms differ with respect to their catalytic properties.[30] The tyrosine in position 108 plays a pivotal role, as the mutation Y to F affects reactions with a number of substrates.[33] The sequence that we have identified by mass spectrometry is identical to the nonmutated isoform designed as GSTP1 A.[30] It is unclear whether the distribution of the different GSTP1 alleles in the population correlates with different forms of cancer.[34–37] A recent study has noted that GSTP null mice have a higher tendency to tumor formation when exposed to mutagens. Thus, GSTP may play a role not only in the inactivation of anticancer drugs but also in the detoxification of mutagens.[38] Interestingly, we did not observe any substantial alterations of GSTP1 expression in proliferating or non-cycling cells, suggesting that the cell cycle-dependent sensitization for RM4819-induced cell death is independent of GSTP1 expression levels.

GSTP1 could interfere with cancer treatment by various mechanisms. Like other GSTs, GSTP1 may inactivate anticancer drugs and thus can be considered as a factor in resistance formation of malignant cells.[39] This fact is used for the design of inactive prodrugs that can be activated by GSTs, mainly GSTA and GSTP.[40] In our case, cells silenced for GSTP1 have a higher sensitivity to

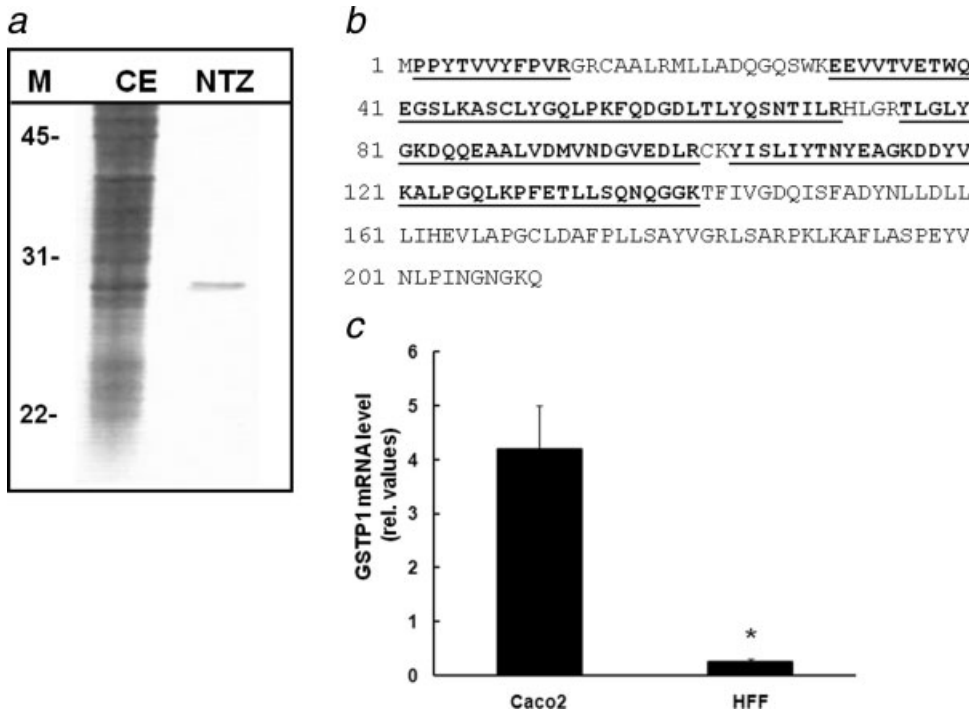

Figure 6 – GSTP1 is a major RM4819-binding protein. (*a*) Affinity chromatography of cell-free extract from 5×10^7 Caco2 cells. Aliquots of fractions were separated by SDS-PAGE. Bands were visualized by silver stain. M, size of marker proteins (kDa); CE, crude extract, NTZ, protein eluted with 1 mM NTZ in PBS. (*b*) Amino acid sequence of the 25-kDa-band that was identified by MS/MS as glutathione-*S*-transferase class Pi isoform P1. The identified peptides are in bold. (*c*) GSTP1 expression in Caco2 and HFF cells. Transcripts of GSTP1 were quantified in relation to actin mRNA. Mean values (±SE) are given for 4 independent experiments. Expression in HFF cells was significantly lower as indicated by an asterisk (*t* test, $p < 0.01$).

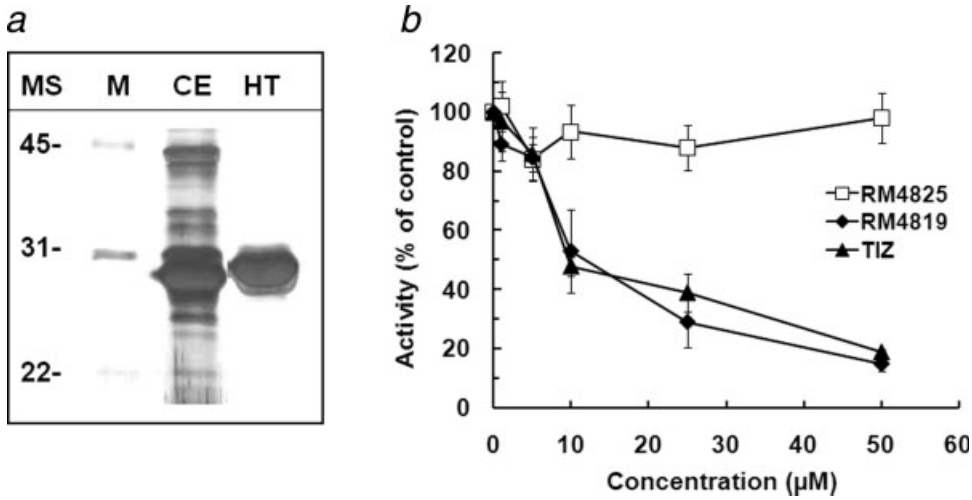

Figure 7 – Expression and assessment of the enzymatic activity of recombinant GSTP1. (*a*) SDS-PAGE of His-tag purified recGSTP1. MS, size of marker proteins, M, marker proteins, CE, crude extract, HT, his-tag purified recGSTP1. (*b*) Activity of recGSTP1 with CDNB as substrate in the presence of TIZ, RM4819, RM4825 (1–50 μM) or DMSO as a solvent control (0 μM). Assays were run in triplicate. Mean values ± SE are given.

doxorubicine. This indicates that detoxification of cancer drugs may indeed be one of the functions of GSTP1. The fact that GSTP1 knockdown cells are less sensitive to RM4819 could be an indication for a different mode of action. For instance, GSTP1 could transform RM4819 into a toxic derivative. Moreover, it is possible that thiazolide binding to GSTP1 triggers cell death in a more indirect way, *e.g.*, by affecting the interaction of GSTP1 and apoptosis-related JNK.[41,42]

Proliferating tumor cell lines like Caco2 are susceptible to thiazolides in a concentration range similar to rapidly proliferating pathogens offering possibilities for tumor treatments using these compounds alone or in combination with radio- or chemotherapy, and thus circumventing drug resistance.[39] It is noteworthy to mention that other antiparasitic compounds are promising anticancer drugs and vice versa. These include serine/threonine and tyrosine kinase inhibitors, synthetic sphingolipid analogues, quassinoids and related

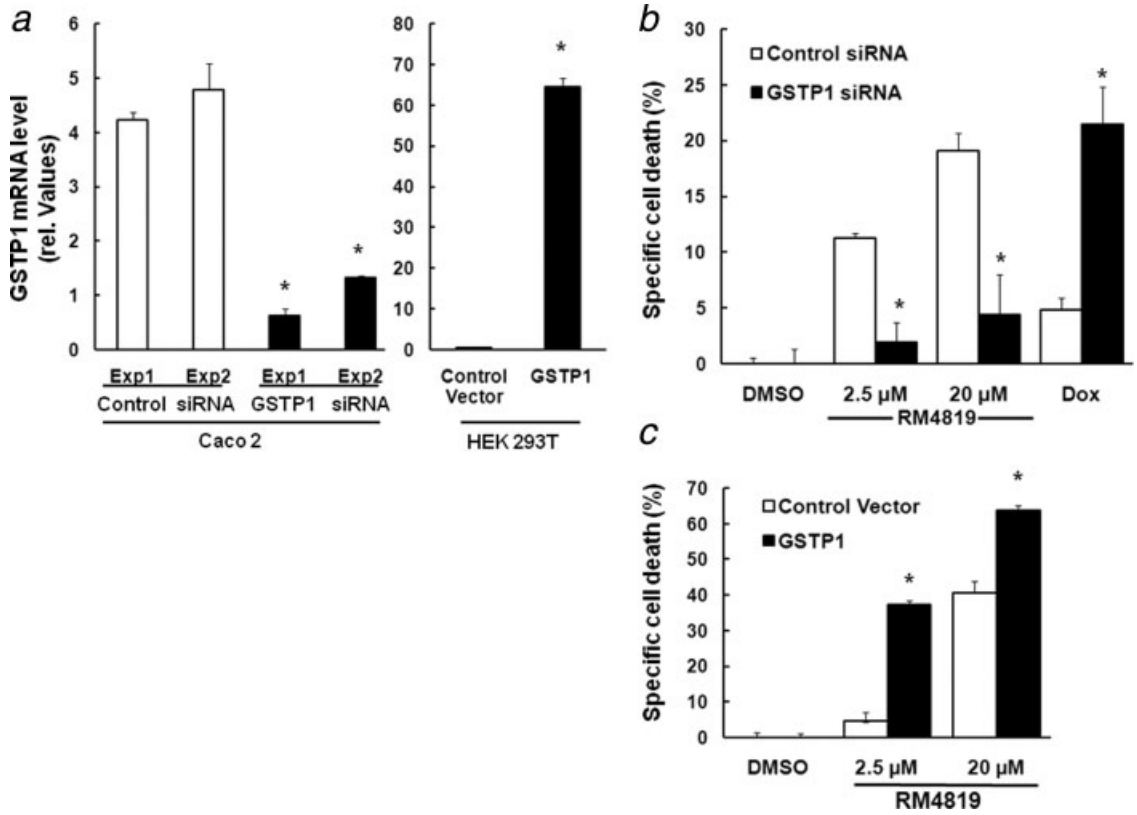

Figure 8 – Sensitivity to RM4819 induced cell death correlates to GSTP1 expression. GSTP1 and siGlo control knockdown were performed in Caco2 cells, and overexpression of GSTP1-GFP was performed in HEK293T cells. Transfected cells were plated in 96-well plates. After 24 h, aliquots of the cells were harvested, RNA was extracted and quantitative RT-PCR was performed. (*a*) Transcripts of GSTP1 were quantified in relation to actin mRNA. Mean values (±SE) are given for triplicates of 2 independent silencing experiment and one overexpression experiment. (*b*) GSTP1and control knockdown cells were challenged with RM4819 or doxorubicine as a positive control for 40 hr. Then, MTT assays were performed in order to determine specific cell death. Mean values (±SE) are given for triplicates. (*c*) HEK293T cells overexpressing GFP-GSTP1 or GFP alone as a negative control were challenged with RM4819. After 40 hr, MTT assays were performed to determine specific cell death. Mean values (± SE) are given for triplicates. Values superscribed by asterisks (*) are significantly different between silenced or overexpressed cells and the respective controls (*t* test, $p < 0.05$).

compounds, artemisin derivatives, proteasome inhibitors, inhibitors of pyrophosphates, inhibitors of polyamine synthesis and alkyllysophospholipid inhibitors.[43] Interestingly, GSTs have been shown to be inhibited by various antimalarial compounds, GSTP1 being the most susceptible.[44] Future work will focus on more details concerning the link between thiazolide drug effects on GSTs, parasite and mammalian (cancer) cell death, and the cellular pathways involved. GSTs may thus be potential drug targets for cancer therapy.

Acknowledgements

We are indebted to Dr. Andrew Stachulski (Department of Chemistry, University of Liverpool) and Dr. Christian Leumann (Department of Biochemistry and Chemistry, University of Berne) for the synthesis of the thiazolides. JM was partially financially supported by the Stanley Thomas Johnson Foundation, and DS received an MD/PhD Fellowship form the Swiss National Science Foundation.

References

1. Hemphill A, Müller J, Esposito M. Nitazoxanide, a broad-spectrum thiazolide anti-infective agent for the treatment of gastrointestinal infections. Expert Opin Pharmacother 2006;7:953–64.
2. Hemphill A, Müller N, Müller J. Structure–function relationship of thiazolides, a novel class of anti-parasitic drugs, investigated in intracellular and extracellular protozoan parasites and larval-stage cestodes. Antiinf Agents Med Chem 2007;6:273–82.
3. Rossignol JF, Maisonneuve H. Nitazoxanide in the treatment of *Taenia saginata* and *Hymenolepis nana*. Am J Trop Med Hyg 1984;33:511–12.
4. Adagu IS, Nolder D, Warhurst D, Rossignol JF. *In vitro* activity of nitazoxanide and related compounds against isolates of *Giardia intestinalis*. *Entamoeba histolytica* and *Trichomonas vaginalis*. J Antimicrob Chemother 2002;49:103–111.
5. Gardner TB, Hill DR. Treatment of Giardiasis. Clin Microbiol Rev 2001;14:114–28.
6. Müller J, Rühle G, Müller N, Rossignol JF, Hemphill A. *In vitro* effects of thiazolides on *Giardia lamblia* WB C6 cultured axenically and in co-culture with Caco2 cells. Antimicrob Agents Chemother 2006;50:162–70.
7. Fox LM, Saravolatz LD. Nitazoxanide: a new thiazolide antiparasitic agent. Clin Inf Dis 2005;40:1173–80.
8. Gilles HM, Hoffman PS. Treatment of intestinal parasitic infections: a review of nitazoxanide. Trends Parasitol 2002;18:95–7.
9. McClure S, Palma K. Treatment of equine protozoal myeloencephalitis with Nitazoxanide. J Eq Vet Sci 1999;19:639–41.
10. White CA, Jr. Nitazoxanide: a new broad spectrum antiparasitic agent. Expert Rev Anti Infect Ther 2004;2:43-9.
11. Rossignol JF, Abu-Zekry M, Hussein A, Santoro MG. Effect of nitazoxanide for treatment of severe rotavirus diarrhoea: randomized double-blind placebo-controlled trial. Lancet 2006;368:124–9.
12. Esposito M, Moores S, Naguleswaran A, Müller J, Hemphill A. Induction of tachyzoite egress from cells infected with the protozoan *Neospora caninum* by nitro- and bromo-thiazolides, a class of broad-spectrum anti-parasitic drugs. Int J Parasitol 2007;37:1143–52.
13. Esposito M, Müller N, Hemphill A. Structure–activity relationships from *in vitro* efficacies of the thiazolide series against the intracellular apicomplexan protozoan *Neospora caninum*. Int J Parasitol 2007; 37:183–90.

14. Esposito M, Stettler R, Moores SL, Pidathala C, Müller N, Stachulski A, Berry NG, Rossignol JF, Hemphill A. *In vitro* efficacies of nitazoxanide and other thiazolides against *Neospora caninum* tachyzoites reveal antiparasitic activity independent of the nitro group. Antimicrob Agents Chemother 2005;49:3715–23.
15. Cortes HCE, Müller N, Esposito M, Leitão A, Naguleswaran A, Hemphill A. *In vitro* efficacy of nitro- and bromo-thiazolyl-salicylamide compounds (thiazolides) against *Besnoitia besnoiti* infection in Vero cells. Parasitology 2007;134:975–85.
16. Broekhuysen J, Stockts A, Lins R, De Graeve J, Rossignol JF. Nitazoxanide: pharmacokinetics and metabolism in man. Int J Clin Pharmacol Ther 2000;38:387–94.
17. Hoffman PS, Sisson G, Croxen MA, Welch K, Dean Harman W, Cremades N, Morash M. Antiparasitic drug nitazoxanide inhibits the pyruvate oxidoreductases of *Helicobacter pylori* and selected anaerobic bacteria and parasites, and *Campylobacter jejuni*. Antimicrob Agents Chemother 2007;51:868–76.
18. Sisson G, Goodwin A, Raudonikiene A, Hughes NJ, Mukhopadhyay AK, Berg DA, Hoffman PS. Enzymes associated with reductive activation and action of nitazoxanide, nitrofurans, and metronidazole in *Helicobacter pylori*. Antimicrob Agents Chemother 2002;46:2116–23.
19. Müller J, Wastling J, Sanderson S, Müller N, Hemphill A. A novel *Giardia lamblia* nitroreductase. GlNR1, interacts with nitazoxanide and other thiazolides. Antimicrob Agents Chemother 2007;51:1979–86.
20. Müller J, Naguleswaran A, Müller N, Hemphill A. Neospora caninum: functional inhibition of protein disulfide isomerase by the broad-spectrum anti-parasitic drug nitazoxanide and other thiazolides. Exp Parasitol 2008;118:80–8.
21. Müller J, Sterck M, Hemphill A, Müller N. Characterization of *Giardia lamblia* WB C6 clones resistant to nitazoxanide and to metronidazole. J Antimicrob Chemother 2007;60:280–7.
22. Guthenberg C, Jensson H, Nystrom L, Osterlund E, Tahir MK, Mannervik B. Isoenzymes of glutathione transferase in rat kidney cytosol. Biochem J 1985;230:609–15.
23. Mannervik B, Alin P, Guthenberg C, Jensson H, Tahir MK, Warholm M, Jörnvall H. Identification of three classes of cytosolic glutathione transferase common to several mammalian species: correlation between structural data and enzymatic properties. Proc Natl Acad Sci USA 1985;82:7202–6.
24. Tew KD. Glutathione-associated enzymes in anticancer drug resistance. Cancer Res 1994;54:4313–4320.
25. Hemphill A, Croft SL. Electron microscopy in parasitology. In: Rogan PM, ed. Analytical parasitology. Heidelberg: Springer Verlag, 1997:227–68.
26. Martin SJ, Reutelingsperger CP, McGahon AJ, Rader JA, van Schie RC, LaFace DM, Green DR. Early redistribution of plasma membrane phosphatidylserine is a general feature of apoptosis regardless of the initiating stimulus: inhibition by overexpression of Bcl-2 and Abl. J Exp Med 1995;182:1545–56.
27. Corazza N, Jakob S, Schaer C, Frese S, Keogh A, Stroka D, Kassahn D, Torgler R, Mueller C, Schneider P, Brunner T. TRAIL receptor-mediated JNK activation and Bim phosphorylation critically regulate Fas-mediated liver damage and lethality. J Clin Invest 2006;116:2493–9.
28. Laemmli UK. Cleavage of structural proteins during the assembly of the head of bacteriophage T4. Nature 1970;227:680–5.
29. Blum H, Beier H, Gross HJ. Improved silver staining of plant proteins. RNA and DNA in polyacrylamide gels. Electrophoresis 1987;8:93–9.
30. Ali-Osman F, Akande O, Antoun G, Mao JX, Buolamwini J. Molecular cloning, characterization, and expression in *Escherichia coli* of full-length cDNAs of three human glutathione *S*-transferase Pi gene variants. J Biol Chem 1997;272:10004–12.
31. Habig WH, Pabst MJ, Jakoby WB. Glutathione-*S*-transferases. The first enzymatic step in mercapturic acid formation. J Biol Chem 1974;249:7130–9.
32. Parkin DP. Purine-specific nucleoside *N*-ribohydrolase from *Trypanosoma brucei brucei*. J Biol Chem 1996;271:21713–19.
33. Lo Bello M, Oakley AJ, Battistoni A, Mazzetti AP, Nuccetelli M, Mazzarese G, Rossjohn J, Parker MW, Ricci G. Multifunctional role of Tyr 108 in the catalytic mechanism of human glutathione transferase P1–1. Crystallographic and kinetic studies on the Y108F mutant enzyme. Biochemistry 1997;36:6207–17.
34. Jiao L, Bondy ML, Hassan MM, Chang DZ, Abbruzzese JL, Evans DB, Smolensky MH, Li D. Glutathione *S*-transferase gene polymorphisms and risk and survival of pancreatic cancer. Cancer 2007;109:840–8.
35. Lu C, Spitz MR, Zhao H, Dong Q, Truong M, Chang JY, Blumenschein GR, Hong WK, Wu X. Association between glutathione *S*-transferase pi polymorphisms and survival in patients with advanced nonsmall cell lung carcinoma. Cancer 2006;106:441–7.
36. Schneider J, Bernges U, Philipp M, Woitowitz HJ. GSTM1, GSTT1, and GSTP1 polymorphism and lung cancer risk in relation to tobacco smoking. Cancer Lett 2004;208:65–74.
37. Wrensch M, Kelsey KT, Liu M, Miike R, Moghadassi M, Aldape K, McMillan A, Wiencke JK. Glutathione-*S*-transferase variants and adult glioma. Cancer Epidemiol Biomarkers Prev 2004;13:461–7.
38. Ritchie KJ, Henderson CJ, Wang XJ, Vassieva O, Carrie D, Farmer PB, Gaskell M, Park K, Wolf CR. Glutathione transferase π plays a critical role in the development of lung carcinogenesis following exposure to tobacco-related carcinogens and urethane. Cancer Res 2007;67:9248–57.
39. Kruh GD. Introduction to resistance to anticancer agents. Oncogene 2003;22:7262–4.
40. Rooseboom M, Commandeur JNM, Vermeulen NPE. Enzyme-catalyzed activation of anticancer prodrugs. Pharmacol Rev 2004;56:53–102.
41. Adler V, Yin Z, Fuchs SY, Benezra M, Rosario L, Tew KD, Pincus MR, Sardana M, Henderson CL, Wolf CR, Davis RJ, Ronai Z. Regulation of JNK signaling by GSTp. EMBO J 1999;18:1321–34.
42. Turella P, Cerella C, Filomeni G, Bullo A, De Maria F, Ghibelli L, Ciriolo MR, Cianfriglia M, Mattei M, Federici G, Ricci G, Caccuri AM. Proapoptotic activity of new glutathione *S*-transferase inhibitors. Cancer Res 2005;65:3751–61.
43. Klinkert MQ, Heussler V. The use of anticancer drugs in antiparasitic chemotherapy. Mini Rev Med Chem 2006;6:131–43.
44. Mukanganyama S, Widersten M, Naik YS, Mannervik B, Hasler JA. Inhibition of glutathione-*S*-transferases by antimalarial drugs possible implications for circumventing anticancer drug resistance. Int J Cancer 2002;97:700–5.